Numerical study on the influence of excavation depth to pile length ratio on a pile group adjacent to an excavation

M.Shakeel, J.Wei & C.W.W.Ng
Dept. of Civil and Environmental Engineering, Hong Kong Univ. of Science and Technology, Clear Water Bay, Kowloon, HKSAR

ABSTRACT
Excavation induced soil movements and stress relief can influence the serviceability of adjacent structures. Most of the previous studies investigated excavation effects on pile lateral movements and bending moments. However, the influence of excavation depth to pile length ratio on settlement and tilting of pile group is not fully understood. By using a validated finite element model, the influence of excavation depth to pile length ratio (H_e/L_p) and relative density of sand (*Dr*) on an existing adjacent pile group are investigated. An advanced sand hypoplastic constitutive model considering small strain stiffness was adopted.

RÉSUMÉ
Les mouvements du sol induits par l'excavation et le soulagement des contraintes peuvent influencer l'état de fonctionnement des structures adjacentes. La plupart des études précédentes ont étudié les effets de l'excavation sur les mouvements latéraux des pieux et les moments de flexion. Cependant, l'influence de la profondeur d'excavation sur le rapport de la longueur de la pile sur le tassement et l'inclinaison du groupe de pieux n'est pas entièrement comprise. À l'aide d'un modèle d'éléments finis validé, on étudie l'influence de la profondeur d'excavation sur le rapport de longueur des pieux (He / Lp) et la densité relative du sable (Dr) sur un groupe de pieux adjacent existant. Un modèle constitutif hypoplasique de sable avancé tenant compte de la faible raideur de la déformation a été adopté.

1. INTRODUCTION

The development of underground space induces ground movements and stress relief in the surrounding soil, which might affect the existing piled supporting structures (Finno et al. 1991) and (Goh et al. 2003). Most of the earlier researchers estimated the buildings settlement and tilting considering wall movements and ground surface settlement trough using empirical approaches.

Field studies (Finno et al. 1991 and Tan et al. 2016), centrifuge modeling (Ng et al. 2017 and Leung et al. 2000) and numerical studies (Poulos and Chen 1997) were conducted to investigate the excavation induced lateral pile movements and bending moments with the advancement of the excavation. Ng et al. 2017 investigated the settlement of single pile adjacent to excavation in the sand by centrifuge modeling. This study was limited to excavation depth to pile length ratio of 0.4. Korff et al. 2016 revealed that soil movements and shaft and end bearing capacities had a significant influence on the pile settlement due to excavation. The influence of stress relief along the pile shaft and below the pile toe was not considered. The response of a pile group with higher values of H_e/L_p ratio (1 and above) requires more attention to study the settlement and tilting mechanism of pile group adjacent to a deep excavation.

This study investigated the influence of excavation depth to pile length ratio on excavation induced pile group settlement and tilting by three dimensional numerical analyses. Moreover, the influence of relative densities of sand (*Dr*) on excavation induced pile group settlement and tilting were also presented.

2. THREE DIMENSIONAL NUMERICAL ANALYSES

Three dimensional numerical studies were performed to investigate the response of an elevated pile group adjacent to a deep excavation using Plaxis 3D (Brinkgreve et al. 2015) software package. In this study influence of excavation depth and soil relative density were examined.

2.1. Numerical analyses plan

The numerical analyses plan was designed to study the influence of excavation level to pile toe (He/Lp) and influence elative density of sand (D_r) (varying relative density from 30% to 90%). In all the analyses final excavation depth (H_e) was 28m and props were assigned 8.75m and 4m center to center spacing in the a horizontal and vertical direction respectively. Elevated 2x2 pile group was considered at a 3m horizontal distance from the wall. The pile diameter (d_p) and pile length (L_p) was 1.25m and 20m respectively. The center to center distance between the piles was three times pile diameter (3.75m). Each depth of excavation was considered as independent final excavation (H_e) as wall penetration depth (H_p) does not affect wall movement and surface settlement of adjacent soil (St John et al. 2005). A typical geometry selected for this study is shown in Figure 1.

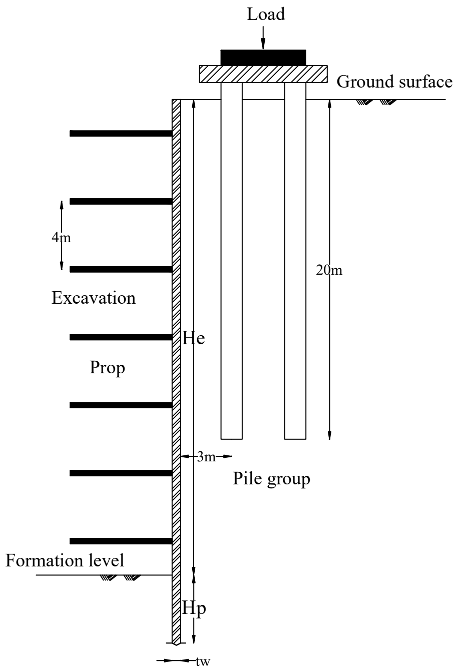

Figure 1 Typical geometry adopted in this study

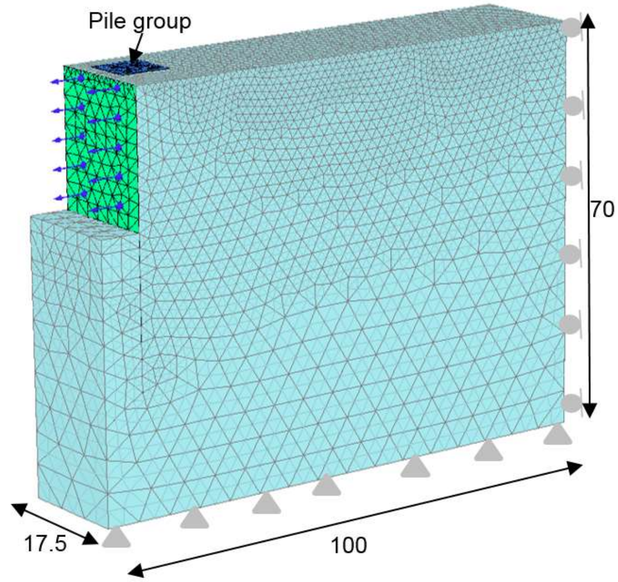

Figure 2 Three dimensional finite element mesh and boundary conditions adopted in this study

2.2. Finite element mesh and constitutive model

Figure 2 shows the three dimensional finite element mesh and boundary conditions used in this study. Soil and pile were modeled 10 nodes tetrahedral solid element. Half of the excavation width (B=6m) was considered due to symmetry. The size of the model was large enough to minimize the boundary effects and considered the influence zone of excavation. Props were modeled 3-node line element. Retaining wall and pile cap were simulated as 6-node plate element. Wall and pile interface was modeled using a 12-node interface element that is built-in available in Plaxis-3D. It consists of a pair of nodes, which is compatible with a 6-node triangular side of soil element or plate element (Brinkgreve et al. 2015).

All the vertical sides were restrained in the horizontal direction by assigning roller support. The model base was fixed in both horizontal and vertical direction by providing pin support.

To model the non-linear soil behavior of Tayoura sand an advanced hypo-plasticity model considering small strain stiffness (von Wolffersdorff 1996 and Niemunis and Herle 1997) was adopted in this numerical study. Basic hypoplastic soil model parameters (h_s, n, e_{do}, e_{co}, e_{io} and ϕ') were obtained based on procedure adopted by Herle and Gudehus (1999). Another two parameters (α and β) were obtained by regression analyses of triaxial test results.

Table 1. Parameters adopted for the numerical study

Parameter	Value
Critical friction angle, ϕ'_c (°)	31
Critical friction angle, h_s (GPa)	2.6
Exponent, n	0.27
Minimum void ratio at zero pressure, e_{d0}	0.61
Critical void ratio at zero pressure, e_{c0}	0.98
Maximum void ratio at zero pressure, e_{i0}	1.1
Exponent, α	0.14
Exponent, β	3.5
Parameters controlling initial shear modulus upon 180° strain path reversal, m_R	8
Parameters controlling initial shear modulus upon 90° strain path reversal, m_T	4
Size of elastic range, R	$2x10^{-5}$
Parameters controlling degradation rate of stiffness with strain, β_r	0.1
Parameters controlling degradation rate of stiffness with strain, χ	1
Coefficient of at-rest earth pressure K_o	0.5

Intergranular strain parameters (m_T, m_R, R, χ and β_R) were used with the basic hypoplastic sand model to incorporate strain dependence and path dependence of soil stiffness(Niemunis and Herle 1997). The adopted soil parameters in this study are summarized in Table 1 and the calibration of the model parameters was presented in Ng et al. 2017.

2.3. Numerical modeling procedures

Initial stress conditions were simulated by applying K_o conditions. Wished-in-place pile group subjected to working load was considered before the commencement of excavation. Bottom-up excavation procedures were adopted. In all the stages struts were installed 1m above the excavation.

3. NUMERICAL BACK ANALYSES OF CENTRIFUGE TEST

3.1. Description of centrifuge test

Centrifuge model test was carried out in the Geotechnical Centrifuge Faculty at the Hong Kong University of Science and Technology. The response of elevated floating pile group (2x2) was investigated adjacent to multi-strutted deep excavation in dry Toyoura sand. The relative density of the sand was 70% which was prepared by dry pluviation technique. The test was performed at 50g level. The final depth of excavation was 8m in the prototype. Pile group was placed 3m from the wall and the piles toes were placed 20m below the ground surface. Retaining wall thickness was 4mm in model scale which simulates the sheet pile and supported by two level of struts. A typical centrifuge model package is shown in Figure 3. The excavation was simulated by draining $ZnCl_2$ heavy fluid having same unit weight as soil. The details of modeling procedure were presented in (Ng et al. 2017).

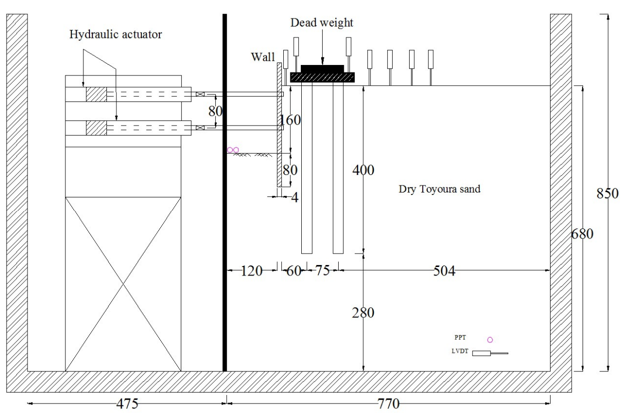

Figure 3 Centrifuge model package of pile group adjacent to excavation (all the dimensions are in mm)

3.2. Comparison of measured and computed results

Figure 4a and 4b shows the measured and computed pile group settlement and tilting respectively adjacent to the multi-strutted deep excavation. Pile group settlement is normalized by the pile diameter and presented in percentage. It shows that pile group settlement increases with the increase of excavation depth. Figure 4b shows the pile group tilting due to adjacent excavation. Tilting of pile group continuously increases with the excavation depth. Initially computed settlement and tilting were lower than the measured but at the end of excavation computed and measured values were match with each other. Overall it shows that adopted finite element modeling approach using hypoplastic soil model can predict the settlement and tilting response of floating pile group adjacent to the deep excavation. In this study, similar modeling approach and constitutive model were used to conduct the parametric study.

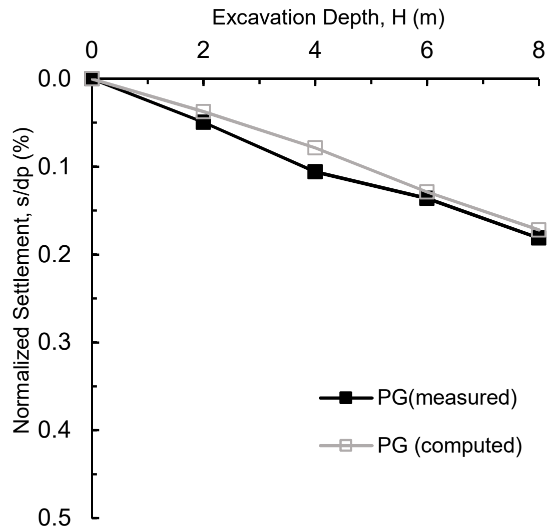

(a) Pile group settlement

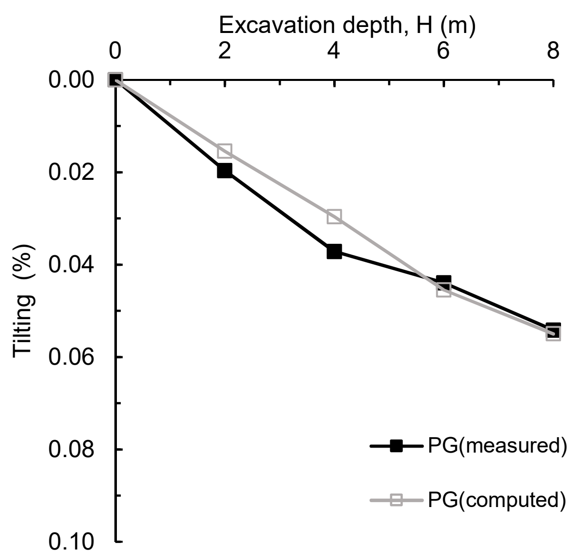

(b) Pile group tilting

Figure 4 Measured and computed pile group response

4. INTERPRETATION OF COMPUTED RESULTS

4.1. Excavation induced soil and pile group settlement and tilting

Figure 5 shows the excavation induced greenfield ground surface settlement with the horizontal distance from the wall. Ground surface settlement and distance from the wall are normalized with final excavation depth (H_e=28m). It shows that ground surface settlement increases with the decrease of soil relative density. The maximum ground settlement was 0.08%, 0.14 and 0.25%H_e corresponding to dense, medium and loose sand respectively. Moreover, the distance of maximum ground settlement increases with the decrease of relative density.

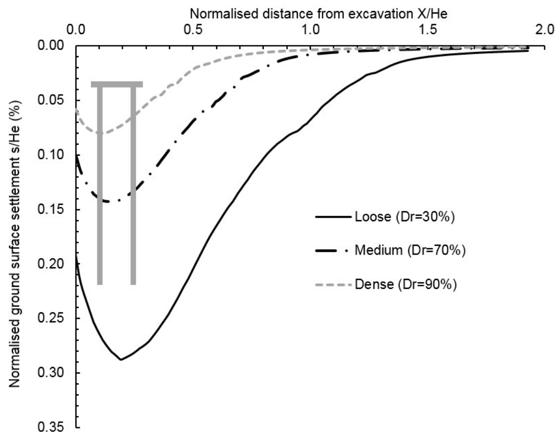

Figure 5 Greenfield ground surface settlement

Figure 6a shows the incremental pile group settlement with the advancement of excavation. Excavation depth (H_e) is normalized by pile length (L_p) and pile group settlement is normalized by pile diameter (d_p). Moreover, the influence of relative density on pile group settlement is also included in the figure. Wall embedded depth has a negligible effect on the wall movement. Therefore, results from intermediate stages of excavation can be used as shallower excavation depths. It shows that pile group settlement continuously increases with the increase of excavation depth for all the relative densities. Moreover, the rate of the settlement also increases with the excavation depth. It is because of the decrease in soil stiffness due to stress relief with the advancement of the excavation. Pile group experiences maximum settlement when the soil density is minimum. It is because of soil stiffness decreases significantly with the decrease of sand relative density.

Figure 6b shows the computed pile group tilting with the excavation depth to pile length ratio (H_e / L_p). Tilting towards the excavation is taken as positive and vice versa. Tilting is defined as the ratio of the differential settlement between the pile cap edges to distance between pile cap edges and presented in percentage. For a dense sand, (D_r=90%) tilting of the pile group is continuously increases with excavation. The rate of tilting increases till H_e/L_p is 1 and decreases with the further advancement of excavation. For medium dense sand tilting increases upto H_e/L_p is 0.9 and then continuously decreases till the H_e/L_p 1.4. For loose sand the trend of pile group tilting is unexpected. Initially tilting is positive and increases till the excavation depth to pile length ratio 0.5 and afterwards, it decreases continuously. There is no tilting when the excavation depth reached to pile toe level (H_e/L_p=1). Further advancement of excavation induced negative pile group tilting (away from the excavation). The maximum tilting induced 0.09% at the end of excavation (H_e/L_p =1.4). The trend of tilting can be explained by looking into ground settlement as shown in Figure 5. For medium and dense sand front pile located in a higher settlement zone than the rear pile, resulting tilting towards the excavation. For loose sand the distance of maximum surface settlement increases from the wall and rear pile experience higher soil movements, resulting pile group tilting away from the excavation.

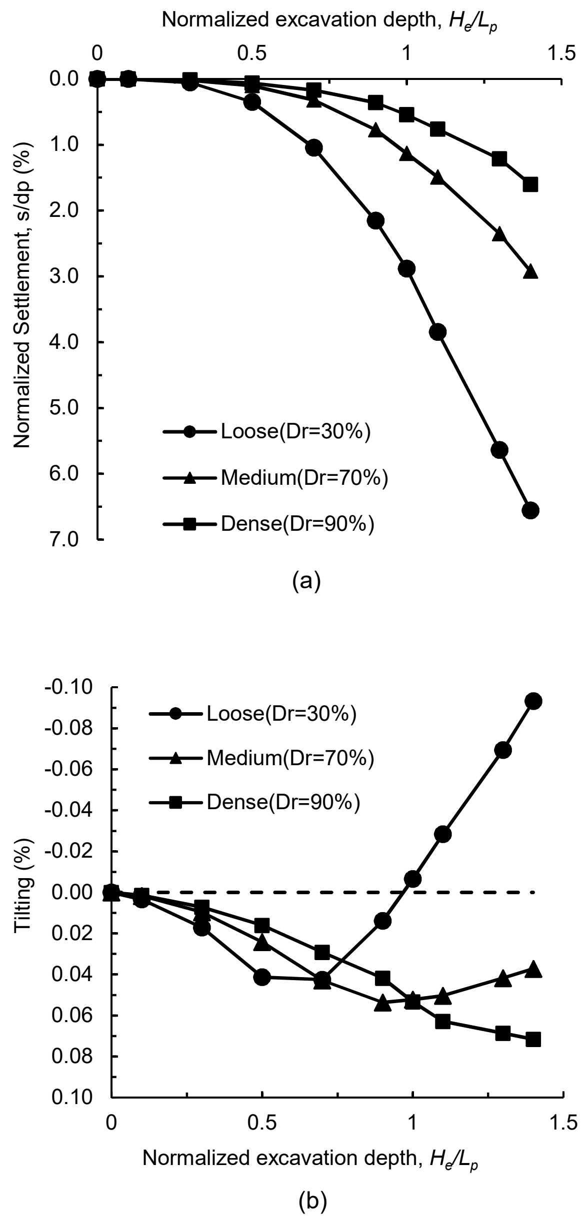

Figure 6 Influence of excavation depth to pile length ratio (H_e/L_p) on (a) Induced pile group settlement (b) tilting of the pile group

4.2. Normal stresses acting on the pile shaft

Figure 7a and 7b show the computed normal stresses acting on the pile shaft for the front (P1) and rear (P2) piles at different H_e/L_p respectively. The sand relative density was 70% which represent medium dense sand. The earth pressure at rest (K_o) and Rankine earth pressure lines (K_a and K_p) are also included as reference lines.

It can be seen that initial pressure distribution follows the K_o line for both the piles. As the excavation proceeded normal stress acting on the piles decreases. When H_e/L_p was 0.5 (excavation depth was at the mid-depth of the pile) normal stress decreases (less than Rankine active earth pressure) in the upper part of the pile while in the lower part of the pile (H_e/L_p 0.7 to 1.0) it followed the K_o line. This implies that in the upper part of the mobilized shaft resistance decreased. While H_e/L_p was 1.0 and 1.4 normal stresses becomes uniform along the pile depth except upper part and lower part of the pile. In the upper part of the pile normal stress approaches Rankine passive pressure line (K_p). This kind of pressure distribution is due to the arching mechanism behind the multi-propped deep excavation.

Figure 7b shows that the reduction in normal stress is lesser in the upper part of the pile while it decreases below the K_a line from Z/L_p >0.4. The reduction of normal stresses along the P2 pile shaft is lesser than the P1 pile shaft. This is because of shielding effect provided by the front pile to rear pile. The resulting nonuniform stress reduction along both the piles contribute towards tilting of the pile group. Moreover, shaft capacity of the pile depends on the normal stresses acting on the pile. Reduction of normal horizontal stress on the pile cause reduction in shaft resistance. This implies that influence of normal stress reduction due to excavation cannot be ignored on the pile group settlement.

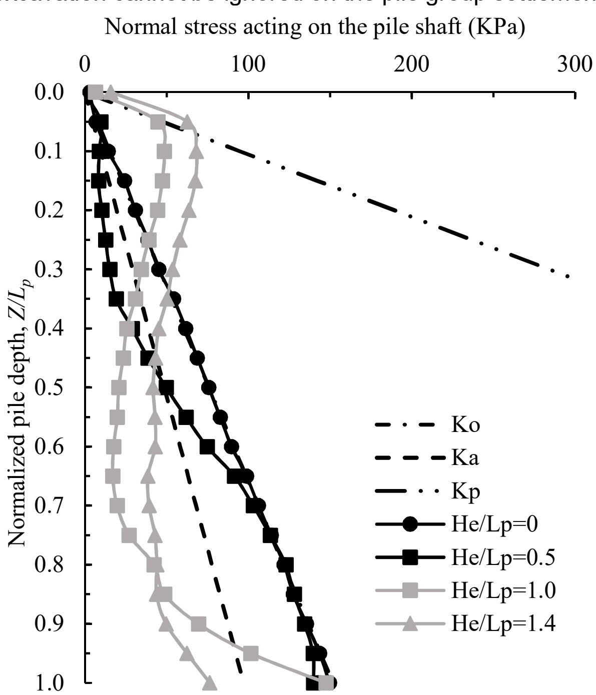

(a) P1 pile

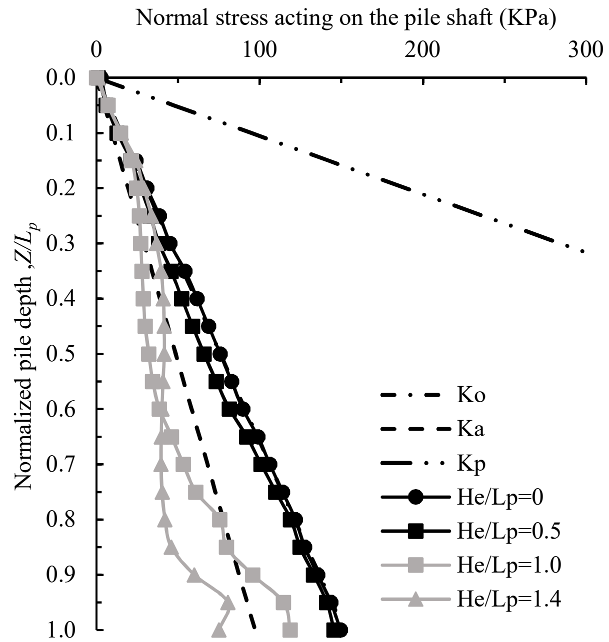

(b) P2 pile

Figure 7 Excavation induced stress release on the pile shaft

4.3. Stress paths of soil elements underneath the pile toe

Figure 8 shows the stress paths of the soil elements underneath the pile toes of both the front (P1) and rear pile (P2) with the advancement of excavation. The critical state line and K_o line are also included for reference. Load (P) represents the stress state of the soil element after the application of axial load. E_i shows the stress level of the soil element when the excavation depth was 'i' m.

It can be seen that initial stress state of the soil element follows the K_o line. Deviatoric stress (q) and mean effective stress (p') are increased after the application of an applied load of soil element and the stress state of the soil element moving towards the critical state line. For the soil element underneath the front pile toe p' and q increases with the advancement of the excavation till the end of 22m excavation. It can be attributed that base resistance is mobilized with the excavation due to downward load transfer from the pile shaft to the pile toe. However, p' decreased after 20m of excavation till the end of excavation. It is attributed that stress relief beneath the pile toe and mobilization of shaft resistance in the upper part of the pile toe. It can also be seen that normal stresses acting on the pile shaft increase in the upper part due to arching effect. Moreover, soil element approaches to the critical state line which shows the failure of soil beneath the pile toe. In contrast to the front pile, both the effective stress and deviatoric stress increases continuously with the advancement of the excavation till the end of excavation. It shows that load is continuously transferred to the pile toe. Stress path for both the soil elements beneath the pile toes implies differential settlement of the piles. It also implies that when the excavation depth is closer or higher than the pile toe there is a reduction of end bearing resistance and potential of soil failure below the pile toe.

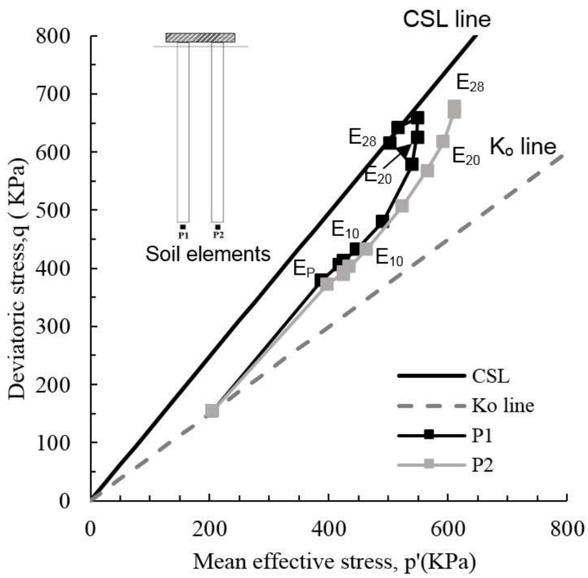

Figure 8 Stress path of the soil element below the pile toe due to excavation

5. CONCLUSIONS

Based on the three dimensional numerical analyses and selected geometry, following conclusions may be drawn:

a. Excavation induced pile group settlement increases with the advancement of excavation. The magnitude of pile group settlement depends on the relative density of sand (*Dr*) and H_e/L_p ratio. For a given geometry and excavation depth, excavation induced pile group settlement decreases with an increase of *Dr*. This is because denser sand has a higher soil stiffness resulting in smaller soil movements, which decreases the pile group settlement.

b. In contrast to the pile group settlement, pile group tilting does not follow any trend with the excavation depth for all the *Dr* considered. For loose sand, pile group tilts towards and away from the excavation at H_e/L_p of 0.5 and 1.0 respectively. For *Dr* of 90% tilting is continuously increases towards the excavation with the increase of H_e/L_p.

c. Normal stresses acting on the pile shaft decreases at H_e/L_p of 0.5 along the pile shaft while it increases in the upper part of the pile at H_e/L_p of 1.0 and 1.4. This is because of the arching mechanism behind the multi-strutted retaining wall. Stress relief occurs below the front pile toe after the H_e/L_p is 1.1. Consequently, pile group settles to mobilize shaft resistance. This implies that loss of end bearing should be considered when H_e/L_p is greater than1.0

6. ACKNOWLEDGMENTS

The authors would like to acknowledge the financial support from the Research Grants Council of the HKSAR (General Research Fund project No. 16207414). In addition, the authors would like to acknowledge financial support M-HKUST603/13 provided by Research Grants Council and FP204 by HKUST.

7. REFERENCES

Brinkgreve, R.B.J., Kumarswamy, S., and Swolfs, W.M. 2015. PLAXIS 3D Tutorial Manual.

Finno, R.J., Lawrence, S.A., Allawh, N.F., and Harahap, I.S. 1991. Analysis of performance of pile groups adjacent to deep excavation. Journal of geotechnical engineering, **117**(6): 934–955. doi:10.1061/(ASCE)0733-9410(1991)117:6(934).

Goh, a. T.C., Wong, K.S., Teh, C.I., and Wen, D. 2003. Pile Response Adjacent to Braced Excavation. Journal of Geotechnical and Geoenvironmental Engineering, **129**(4): 383–386. doi:10.1061/(ASCE)1090-0241(2003)129:4(383).

Korff, M., Mair, R.J., and Van Tol, F.A.F. 2016. Pile-Soil Interaction and Settlement Effects Induced by Deep Excavations. Journal of Geotechnical and Geoenvironmental Engineering, **138**(7): 4016034. doi:10.1061/(ASCE)GT.1943-5606.0001434.

Leung, C., Chow, Y., and Shen, R. 2000. Behavior of pile subject to excavation-induced soil movement. Journal of Geotechnical and,. Available from http://ascelibrary.org/doi/abs/10.1061/(ASCE)1090-0241(2000)126:11(947) [accessed 2 December 2016].

Ng, C.W.W., Wei, J., Poulos, H., and Liu, H. 2017. Effects of Multipropped Excavation on an Adjacent Floating Pile. Journal of Geotechnical and Geoenvironmental Engineering, **143**(7): 4017021. doi:10.1061/(ASCE)GT.1943-5606.0001696.

Niemunis, A., and Herle, I. 1997. Hypoplastic model for cohesionless soils with elastic strain range. Mechanics of Cohesive-Frictional Materials, **2**(4): 279–299. doi:10.1002/(SICI)1099-1484(199710)2:4<279::AID-CFM29>3.0.CO;2-8.

Poulos, H.G., and Chen, L.T. 1997. Pile Response Due to Excavation-Induced Lateral Soil Movement. Journal of Geotechnical and Geoenvironmental Engineering, **123**(4): 382–388. doi:10.1061/(ASCE)1090-0241(1997)123.

St John, H.D., Zdravkovic, L., and Potts, D.M. 2005. Modelling of a 3D excavation in finite element analysis. Géotechnique, **55**(7): 497–513. doi:10.1680/geot.2005.55.7.497.

Tan, Y., Huang, R., Kang, Z., and Bin, W. 2016. Covered semi-top-down excavation of subway station surrounded by closely spaced buildings in downtown shanghai: building response. Journal of Performance of Constructed Facilities, **30**(6): 1–26. doi:10.1061/(ASCE)CF.1943-5509.0000892.

von Wolffersdorff, P.A. 1996. Hypoplastic relation for granular materials with a predefined limit state surface. Mechanics of Cohesive-Frictional Materials, **1**(3): 251–271. doi:10.1002/(SICI)1099-1484(199607)1:3<251::AID-CFM13>3.0.CO;2-3.